The Journal of Chemical Physics ARTICLE pubs.aip.org/aip/jcp

Jump discontinuities of finite-basis-set exchange–correlation potentials at atomic nuclei

Cite as: J. Chem. Phys. 161, 124106 (2024); doi: 10.1063/5.0228216
Submitted: 11 July 2024 • Accepted: 5 September 2024 •
Published Online: 23 September 2024

View Online Export Citation CrossMark

Conrad C. Moore and Viktor N. Staroverov[a)]

AFFILIATIONS

Department of Chemistry, The University of Western Ontario, London, Ontario N6A 5B7, Canada

[a)]Author to whom correspondence should be addressed: vstarove@uwo.ca

ABSTRACT

The kinetic energy density of electrons and the gradient of the electron density have pronounced jump discontinuities at the positions of the atomic nuclei in molecules. Certain exact relations then imply that molecular Kohn–Sham exchange–correlation potentials may also be discontinuous at atomic nuclei. Here, we confirm that exchange–correlation potentials derived from Hartree–Fock and correlated wavefunctions within Slater-type basis sets do exhibit such discontinuities. Despite their persistence even in large basis sets, these discontinuities are almost certainly artifacts of basis set finiteness and are expected to disappear in the basis-set limit. The findings imply that imposing electron–nucleus cusp conditions in spherically averaged form may not always be appropriate.

Published under an exclusive license by AIP Publishing. https://doi.org/10.1063/5.0228216

30 September 2024 16:01:33

I. INTRODUCTION

Most electronic structure calculations today are carried out using the approximate Kohn–Sham density-functional theory.[1–3] A density-functional approximation for the exchange–correlation (XC) energy gives rise to the corresponding XC potential, $v_{\rm XC}(\mathbf{r})$, which is used to solve the Kohn–Sham equations.[4] For a given system, the XC potential can be obtained directly from a given electron density[5–10] or from the electronic wavefunction.[11–17] Construction of XC potentials from wavefunctions has the advantage that it gives physically correct (non-oscillatory and non-divergent) XC potentials within Gaussian-type basis sets. Inspection of XC potentials deduced from accurate wavefunctions and electron densities informs the development of density-functional approximations.

One property of exact XC potentials that is taken for granted is their continuity at atomic nuclei. This belief stems from visual inspections of countless XC potentials constructed from accurate electron densities and electronic wavefunctions. Molecular XC potentials obtained in this manner show no obvious signs of being discontinuous at the nuclear positions. Nevertheless, there is a distinct possibility that such discontinuities may exist.

First, XC potentials can be written exactly in terms of interacting and noninteracting kinetic energy densities[11–15] that are known to have sharp discontinuities at the atomic nuclei in molecules[18–21] due to the directional dependence of the electron–nucleus cusps of exact wavefunctions.[22–26] According to these exact formulas, the discontinuities of the kinetic energy densities should lead to discontinuities of XC potentials themselves, unless some counter-intuitive cancellation occurs. Second, the values of exact XC potentials at a nuclear cusp are not easy to ascertain by fitting potentials to electron densities,[6–10,27] so it is conceivable that the discontinuities have been overlooked. Third, if the hypothetical discontinuities of XC potentials are small, they would not be discovered in calculations using Gaussian-type orbitals (GTOs) because GTOs are cuspless. To see these discontinuities, one must employ Slater-type orbitals (STOs).

Recently, Tribedi *et al.*[28] used the method of Refs. 12 and 15 to construct for the first time molecular XC potentials from electronic wavefunctions expanded in STOs. These workers did not specifically look for discontinuities of $v_{\rm XC}(\mathbf{r})$, but some of their results (e.g., Fig. 5 of Ref. 28) could be interpreted in favor of the discontinuity hypothesis. Our own recent work[21] suggested that any discontinuities of $v_{\rm XC}(\mathbf{r})$, if they exist, would likely be small on the scale of the value of $v_{\rm XC}(\mathbf{r})$ at a nucleus. In other words, discontinuities of XC potentials would be easy to miss or mistake for something else if one is not looking for them specifically.

In this work, we show that the jump discontinuities of $v_{\rm XC}(\mathbf{r})$ are real within finite STO basis sets and that their presumed disappearance in the basis-set limit implies nontrivial relations between the interacting and noninteracting kinetic energy densities.

Published under an exclusive license by AIP Publishing

II. METHODS

A. Working equations

We construct XC potentials from electronic wavefunctions using two different exact formulas that give slightly different results within a given finite basis set. The first formula is[12]

$$v_{\rm XC}^{\rm I}(\mathbf{r}) = v_{\rm XC}^{\rm hole}(\mathbf{r}) + \bar{\epsilon}^{\rm KS}(\mathbf{r}) - \bar{\epsilon}^{\rm WF}(\mathbf{r}) + \frac{\tau^{\rm WF}(\mathbf{r})}{\rho^{\rm WF}(\mathbf{r})} - \frac{\tau^{\rm KS}(\mathbf{r})}{\rho^{\rm KS}(\mathbf{r})}. \quad (1)$$

Here, $\tau^{\rm WF}(\mathbf{r})$ and $\tau^{\rm KS}(\mathbf{r})$ are the interacting and noninteracting (Kohn–Sham) "positive-definite" kinetic energy densities, which can be both written as

$$\tau(\mathbf{r}) = \frac{1}{2}\sum_i n_i |\nabla\phi_i(\mathbf{r})|^2, \quad (2)$$

where $\phi_i(\mathbf{r})$ are natural or Kohn–Sham orbitals, respectively, and n_i are the orbital occupation numbers ($0 \le n_i \le 2$). The denominators $\rho^{\rm WF}(\mathbf{r})$ and $\rho^{\rm KS}(\mathbf{r})$ in Eq. (1) are the electron densities derived from the interacting and noninteracting wavefunctions, respectively. The definitions of all other quantities appearing in Eq. (1) may be found in Ref. 29. It is essential that $v_{\rm XC}^{\rm hole}(\mathbf{r})$, $\bar{\epsilon}^{\rm KS}(\mathbf{r})$, and $\bar{\epsilon}^{\rm WF}(\mathbf{r})$ do not depend on orbital gradients and, therefore, are continuous everywhere.

The second formula is[15]

$$v_{\rm XC}^{\rm II}(\mathbf{r}) = v_{\rm XC}^{\rm hole}(\mathbf{r}) + \bar{\epsilon}^{\rm KS}(\mathbf{r}) - \bar{\epsilon}^{\rm WF}(\mathbf{r}) + \frac{\tau_P^{\rm WF}(\mathbf{r})}{\rho^{\rm WF}(\mathbf{r})} - \frac{\tau_P^{\rm KS}(\mathbf{r})}{\rho^{\rm KS}(\mathbf{r})}, \quad (3)$$

where $\tau_P^{\rm WF}(\mathbf{r})$ and $\tau_P^{\rm KS}(\mathbf{r})$ are the interacting and noninteracting Pauli kinetic energy densities, respectively. Each of these is related to the corresponding "positive-definite" $\tau(\mathbf{r})$ by

$$\tau_P(\mathbf{r}) = \tau(\mathbf{r}) - \tau_W(\mathbf{r}), \quad (4)$$

where

$$\tau_W(\mathbf{r}) = \frac{|\nabla\rho(\mathbf{r})|^2}{8\rho(\mathbf{r})} \quad (5)$$

is the Weizsäcker kinetic energy density.

Both Eqs. (1) and (3) must be used in a self-consistent manner, i.e., by starting with fixed wavefunction ingredients and solving the Kohn–Sham equations iteratively until the corresponding Kohn–Sham ingredients stop varying. If these iterations were carried out using a complete basis set, the densities $\rho^{\rm WF}(\mathbf{r})$ and $\rho^{\rm KS}(\mathbf{r})$ would coincide at convergence,[15,30] and we would have

$$v_{\rm XC}^{\rm I}(\mathbf{r}) = v_{\rm XC}^{\rm II}(\mathbf{r}). \quad (6)$$

Within finite basis sets, this equality holds only approximately,[12,15] which is why it is essential to treat $\rho^{\rm WF}(\mathbf{r})$ and $\rho^{\rm KS}(\mathbf{r})$ as distinct. The extent to which $\rho^{\rm KS}(\mathbf{r})$ deviates from $\rho^{\rm WF}(\mathbf{r})$ at convergence is quantified here using the metric,

$$\Delta_\rho = \frac{1}{N}\int |\rho^{\rm KS}(\mathbf{r}) - \rho^{\rm WF}(\mathbf{r})| d\mathbf{r}, \quad (7)$$

where N is the total number of electrons in the system. Other details of the potential construction method based on Eqs. (1) and (3) may be found in Ref. 15.

B. Computational details

We implemented Eqs. (1) and (3) within STO basis sets using the Wolfram Language.[31] The electron repulsion integrals over STOs were evaluated analytically using the algorithm of Harris.[32] All other integrals were evaluated numerically using the built-in Wolfram Language function `NIntegrate`, with eight effective digits of accuracy.[31] Our implementation is capable of solving the Hartree–Fock and Kohn–Sham self-consistent field (SCF) equations using the direct inversion in the iterative subspace[33] to accelerate SCF convergence. The Hartree–Fock and Kohn–Sham orbitals are considered converged when the root-mean-square deviation of the current and previous density matrices is less than 10^{-8} atomic units.

We found that the SCF convergence of the Kohn–Sham orbitals is often hindered by numerical artifacts arising at grid points far from the nuclei, where the Kohn–Sham kinetic energy densities are divided by very small $\rho^{\rm KS}(\mathbf{r})$ values. Following Stückrath and Bischoff,[16] we deal with this problem by regularizing the division by $\rho^{\rm KS}(\mathbf{r})$ at every $\mathbf{r}$ through the substitution,

$$\frac{1}{\rho^{\rm KS}(\mathbf{r})} \to \frac{1}{\rho^{\rm KS}(\mathbf{r}) + \epsilon}, \quad (8)$$

where $\epsilon = 10^{-8}$ a.u. This modification has no consequential effect on the value of an XC potential near atomic nuclei, where the density is at least of the order of 10^2 even for light atoms such as Li and B.

The STO basis sets used were those of Ema *et al.*,[34] namely, VB1, VB2, VB3. To give a sense of their quality relative to standard GTO basis sets, the total HF/VB3 energies for the Li_2 and BH molecules are equal to the HF/cc-pV5Z energies within four decimal places (in hartrees).

Jump discontinuities of kinetic energy densities and XC potentials appear only at the positions of the atomic nuclei.[18–21] For diatomic molecules, these jumps vary depending on the direction of going through the nucleus and have the greatest magnitude along the internuclear axis. To quantify the magnitude of a jump of a function $f(\mathbf{r})$ at a particular nucleus in the local coordinate system centered on that nucleus, we use the quantity,

$$\Delta f = \lim_{\mathbf{r}\to+0} f(\mathbf{r}) - \lim_{\mathbf{r}\to-0} f(\mathbf{r}), \quad (9)$$

where $\mathbf{r} \to +0$ means the approach along the internuclear axis from inside the internuclear region, whereas $\mathbf{r} \to -0$ means the approach from outside that region. With this convention, $\Delta f > 0$ when the function $f(\mathbf{r})$ jumps up at the nucleus when going along the internuclear axis toward the center of the bond.

III. RESULTS

A. Discontinuities of XC potentials

We begin by examining the origin of the discontinuities of XC potentials in STO basis sets. Since the quantities $v_{\rm XC}^{\rm hole}(\mathbf{r})$, $\bar{\epsilon}^{\rm KS}(\mathbf{r})$, and $\bar{\epsilon}^{\rm WF}(\mathbf{r})$ are all continuous everywhere, any possible discontinuities of $v_{\rm XC}^{\rm I}(\mathbf{r})$ can arise only from the "positive-definite" kinetic energy densities $\tau^{\rm WF}(\mathbf{r})$ and $\tau^{\rm KS}(\mathbf{r})$. Similarly, any possible discontinuities of $v_{\rm XC}^{\rm II}(\mathbf{r})$ can be caused only by discontinuities of $\tau_P^{\rm WF}(\mathbf{r})$ and $\tau_P^{\rm KS}(\mathbf{r})$. We will use the Li_2 and BH molecules as case studies.

30 September 2024 16:01:33

Published under an exclusive license by AIP Publishing

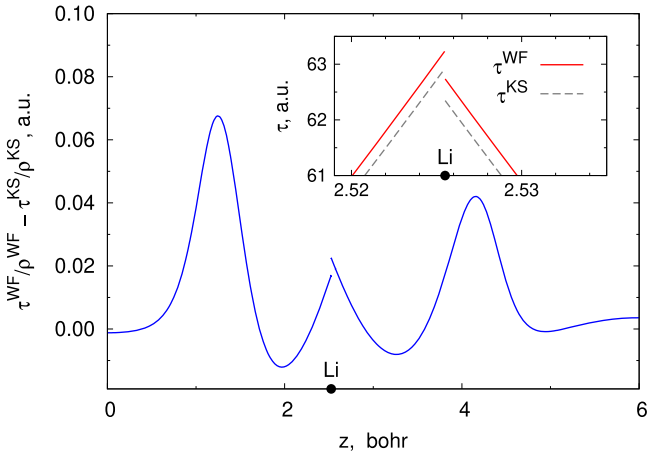


FIG. 1. Discontinuous ingredients of $v_{XC}^{I}(\mathbf{r})$ constructed from the HF/VB3 wavefunction of Li_2 (R = 5.051 bohrs). Each ingredient is plotted along the internuclear axis with the bond midpoint at z = 0.

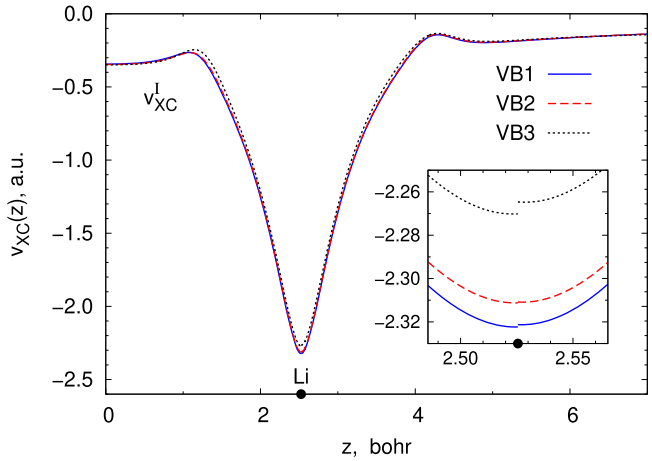


FIG. 3. Potentials $v_{XC}^{I}(\mathbf{r})$ constructed from Hartree–Fock wavefunctions of Li_2 (R = 5.051 bohrs) expanded in various STO basis sets. The potentials are plotted along the internuclear axis with the bond midpoint at z = 0. The inset shows $v_{XC}^{I}(\mathbf{r})$ in the vicinity of the right-side Li nucleus.

The inset of Fig. 1 shows that the kinetic energy densities $\tau^{WF}(\mathbf{r})$ and $\tau^{KS}(\mathbf{r})$ obtained from the HF/VB3 wavefunction of Li_2 are distinct and discontinuous at the nuclei, with jump discontinuities of the order of 1 a.u. along the internuclear axis. These discontinuities do not cancel out and make $v_{XC}^{I}(\mathbf{r})$ discontinuous, as shown in the main plot of Fig. 1. Similar results would be obtained for $\tau_P^{WF}(\mathbf{r})$, $\tau_P^{KS}(\mathbf{r})$, and $v_{XC}^{II}(\mathbf{r})$.

Figure 2 confirms that the overall potential $v_{XC}^{I}(\mathbf{r})$ of Li_2 derived from the HF/VB3 wavefunction is discontinuous at each nucleus. The magnitude of the jump discontinuity of $v_{XC}^{I}(\mathbf{r})$ depends on the direction in which one passes through the nucleus. The jump varies from zero in the direction perpendicular to the internuclear axis to the maximum value of about 0.0055 a.u. along the internuclear axis.

Figures 3–5 compare potentials $v_{XC}^{I}(\mathbf{r})$ and $v_{XC}^{II}(\mathbf{r})$ constructed from Hartree–Fock wavefunctions of Li_2 and BH using different STO basis sets. The discontinuities are present in all cases, although they are relatively small for $v_{XC}^{I}(\mathbf{r})$ and smaller still for $v_{XC}^{II}(\mathbf{r})$. Curiously, the magnitude of the discontinuity of $v_{XC}^{I}(\mathbf{r})$ for Li_2 increases from VB2 to VB3, but decreases for $v_{XC}^{II}(\mathbf{r})$. This shows that numerical evidence alone is insufficient to decide whether the observed discontinuities of $v_{XC}^{I}(\mathbf{r})$ and $v_{XC}^{II}(\mathbf{r})$ would vanish in the basis-set limit.

Jump discontinuities of STO-based XC potentials are not specific to Hartree–Fock wavefunctions. This can be demonstrated for two-electron molecules with only one occupied Kohn–Sham orbital (such as the ground-state H_2). For such systems, the Kohn–Sham ingredients reduce to a constant, and Eq. (3) becomes[35]

$$v_{XC}^{III}(\mathbf{r}) = v_{XC}^{hole}(\mathbf{r}) - \tilde{\epsilon}^{WF}(\mathbf{r}) + \frac{\tau_P^{WF}(\mathbf{r})}{\rho^{WF}(\mathbf{r})} - I, \tag{10}$$

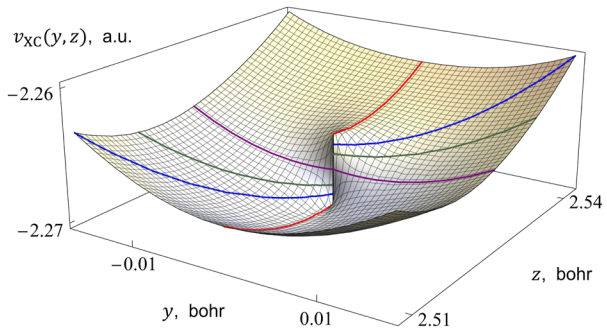


FIG. 2. Behavior of an STO-based $v_{XC}^{I}(\mathbf{r})$ near an atomic nucleus in Li_2 (R = 5.051 bohrs). The potential was derived from the HF/VB3 wavefunction. The internuclear axis is z. The molecule is oriented as in Fig. 1. The curves in color show changes in the potential along four different lines that pass through the nucleus in the yz plane.

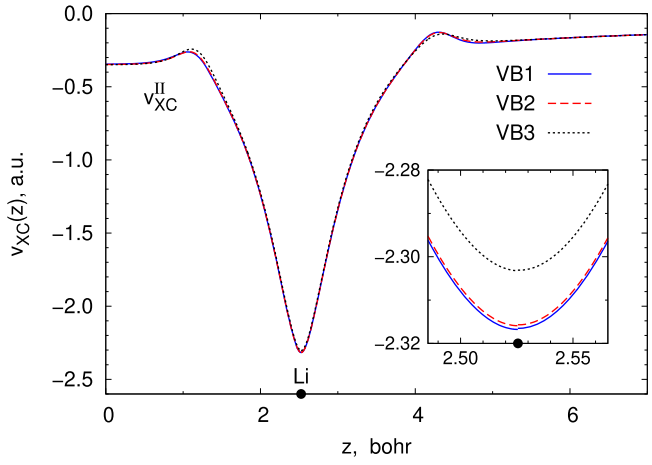


FIG. 4. Same as in Fig. 3, but using Eq. (3) instead of Eq. (1).

30 September 2024 16:01:33

Published under an exclusive license by AIP Publishing

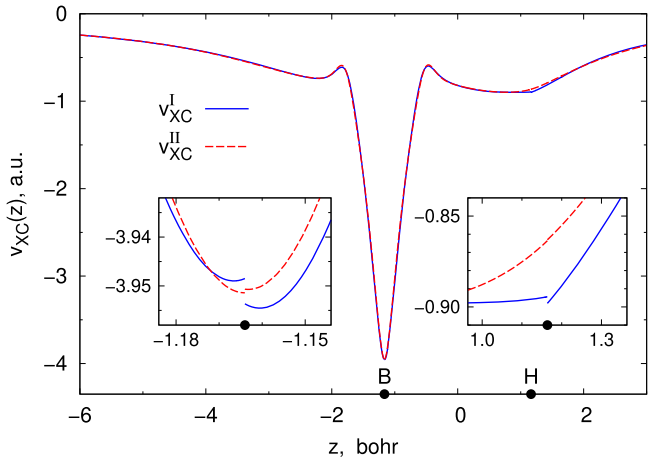


FIG. 5. Potentials $v^{I}_{XC}(\mathbf{r})$ and $v^{II}_{XC}(\mathbf{r})$ constructed from the HF/VB3 wavefunction of BH (R = 2.328 bohrs). The potentials are plotted along the internuclear axis with the bond midpoint at z = 0. The insets show the potentials in the vicinity of each nucleus.

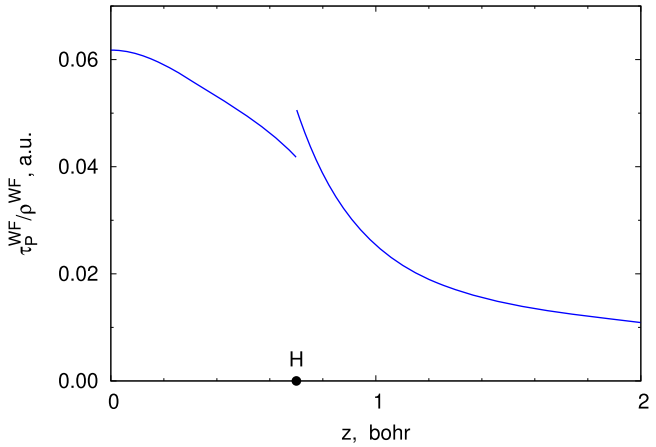


FIG. 6. The ratio $\tau_P^{WF}/\rho^{WF}(\mathbf{r})$ along the internuclear axis of the H_2 (R = 1.4 bohrs) molecule computed from a CI wavefunction.[37] The point z = 0 is the center of the bond. This result implies that the overall potential $v^{III}_{XC}(\mathbf{r})$ is similarly discontinuous.

where I is the first ionization energy of the system. The quantity $\tau_P^{WF}(\mathbf{r})$ is zero for any two-electron closed-shell Hartree–Fock wavefunction, but not for a configuration interaction (CI) wavefunction.[35,36] Thus, whether the exact $v_{XC}(\mathbf{r})$ is continuous or not at the atomic nuclei of H_2 depends entirely on the behavior of $\tau_P^{WF}(\mathbf{r})$.

Figure 6 shows that the ratio $\tau_P^{WF}(\mathbf{r})/\rho^{WF}(\mathbf{r})$ is discontinuous in H_2 for a CI wavefunction expanded in an STO basis set.[37] According to Eq. (10), the corresponding $v_{XC}(\mathbf{r})$ constructed from this wavefunction would also be discontinuous. Whether this discontinuity would persist in the basis-set limit cannot be concluded on the basis of numerical evidence alone.

According to Fig. 6, the Pauli kinetic energy density $\tau_P^{WF}(\mathbf{r})$ is non-negative at the H nucleus in every direction, which means that the spherical average $\bar{\tau}_P^{WF}(0)$ is not zero. This result is at odds with statements found in the older literature but is consistent with more recent reports.[38]

B. Magnitude of the jumps

Table I reports the jump discontinuities of the "positive-definite" and Pauli kinetic energy densities for the Li_2 and BH molecules, along with the discontinuities of the respective $v^{I}_{XC}(\mathbf{r})$ and $v^{II}_{XC}(\mathbf{r})$. The maximum value of each kinetic energy density is included to give a sense of the relative size of the jumps.

The maximum values of $\tau^{WF}(\mathbf{r})$ and $\tau^{KS}(\mathbf{r})$ are large, whereas those of $\tau_P^{WF}(\mathbf{r})$ and $\tau_P^{KS}(\mathbf{r})$ are relatively small. The difference of two large but roughly equal quantities $\tau^{WF}(\mathbf{r})$ and $\tau^{KS}(\mathbf{r})$ varies more unpredictably than the difference of the much smaller $\tau_P^{WF}(\mathbf{r})$ and $\tau_P^{KS}(\mathbf{r})$. This explains why the jump discontinuities of $v^{I}_{XC}(\mathbf{r})$

TABLE I. Maximum values of kinetic energy densities, their jumps, and the jumps of $v_{XC}(\mathbf{r})$ (all in atomic units) at the nuclei of Li_2 and BH computed using Eqs. (1) and (3) from Hartree–Fock wavefunctions expanded in various STO basis sets.

		v^{I}_{XC}					v^{II}_{XC}				
Nucleus	Basis set	max τ^{WF}	max τ^{KS}	$\Delta\tau^{WF}$	$\Delta\tau^{KS}$	Δv_{XC}	max τ_P^{WF}	max τ_P^{KS}	$\Delta\tau_P^{WF}$	$\Delta\tau_P^{KS}$	Δv_{XC}
					Li_2 (R = 5.051 bohrs)						
Li	VB1	63.165	63.241	0.1494	0.1642	−0.0012	0.0016	0.0031	−0.0008	0.0029	−0.0003
	VB2	63.098	63.073	0.1747	0.1801	−0.0004	0.0014	0.0030	−0.0004	0.0027	−0.0002
	VB3	63.241	62.927	0.5027	0.5782	−0.0055	0.0024	0.0044	0.0004	0.0024	−0.0001
					BH (R = 2.328 bohrs)						
B	VB1	904.86	910.28	−7.5711	−7.6707	0.0009	1.4724	1.5576	0.4386	0.1997	0.0033
	VB2	908.98	910.94	−8.2592	−8.2166	−0.0009	1.2695	1.4784	0.0803	0.0287	0.0007
	VB3	909.67	909.63	−8.6440	−8.2887	−0.0052	1.2959	1.6161	0.0122	−0.0410	0.0007
H	VB1	0.3824	0.3511	−0.2481	−0.2473	0.0120	0.0021	0.0027	0.0012	0.0006	0.0014
	VB2	0.3836	0.3878	−0.2583	−0.2760	0.0396	0.0017	0.0019	0.0004	0.0002	0.0003
	VB3	0.3752	0.3950	−0.2464	−0.2508	0.0036	0.0018	0.0023	−0.0009	−0.0007	−0.0005

30 September 2024 16:01:33

Published under an exclusive license by AIP Publishing

in Table I sometimes increase with increasing basis set size, whereas those of $v_{XC}^{II}(\mathbf{r})$ appear to decrease.

C. Density errors

According to Figs. 3–5 and Table I, the finite-basis-set potentials $v_{XC}^{II}(\mathbf{r})$ have smaller discontinuities than $v_{XC}^{I}(\mathbf{r})$ and appear to converge faster with respect to the basis set. Table II reveals that, counterintuitively, the density errors Δ_ρ of $v_{XC}^{I}(\mathbf{r})$ and $v_{XC}^{II}(\mathbf{r})$ are similar. This result is an instructive reminder of the well-known fact that a smoother potential is not necessarily more accurate for the purpose of reproducing a given density.[39,40]

To elaborate on this observation, we plotted the local density error, $|\rho^{KS}(\mathbf{r}) - \rho^{WF}(\mathbf{r})|$, for the BH molecule calculated at the HF/VB3 level (see Fig. 7). The local density error of $v_{XC}^{I}(\mathbf{r})$ along the internuclear axis is greater than that of $v_{XC}^{II}(\mathbf{r})$, as expected. However, Table II shows that the integrated density errors for the two potentials are roughly equal. It appears that the larger jump discontinuity of $v_{XC}^{I}(\mathbf{r})$ affects the density only near the nucleus but does not increase the density error overall.

TABLE II. Hartree–Fock total energies and density errors of molecular XC potentials constructed from Hartree–Fock wavefunctions using various STO basis sets.

		Δ_ρ	
Basis set	E_e (E_h)	v_{XC}^{I}	v_{XC}^{II}
	Li_2 (R = 5.051 bohrs)		
VB1	−14.871 093	0.0051	0.0065
VB2	−14.871 229	0.0049	0.0058
VB3	−14.871 531	0.0044	0.0047
	BH (R = 2.328 bohrs)		
VB1	−25.130 540	0.0078	0.0086
VB2	−25.131 461	0.0048	0.0053
VB3	−25.131 567	0.0041	0.0042

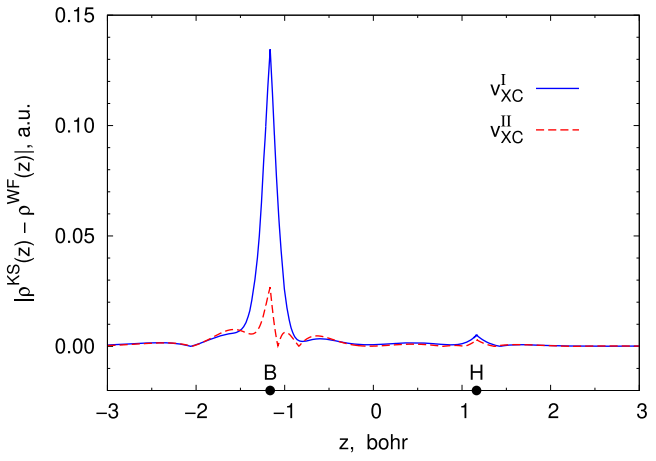


FIG. 7. Local density errors of the XC potentials of Fig. 5. The densities are plotted along the internuclear axis with the bond midpoint at z = 0.

IV. DISCUSSION

The above results demonstrate that molecular XC potentials constructed by Eqs. (1) and (3) using finite STO basis sets are discontinuous at atomic nuclei. Since Eqs. (1) and (3) themselves are not in doubt, one should wonder whether these discontinuities are artifacts of using finite basis sets or a true property of exact XC potentials in the basis-set limit. The latter possibility is not far-fetched in view of Fig. 3, which shows that the magnitude of the jump sometimes increases from a smaller basis set (VB2) to a larger one (VB3).

If XC potentials are indeed continuous in the basis-set limit, then the interacting and noninteracting kinetic energy densities must have the same directional dependence at each nucleus and the same as $\tau_W(\mathbf{r})$. This conclusion, if true, would be astounding because $\tau^{WF}(\mathbf{r})$, $\tau^{KS}(\mathbf{r})$, and $\tau_W(\mathbf{r})$ are generally different functions of $\mathbf{r}$ with different values at a nucleus.[41]

To settle the matter requires analyzing the directional dependence of the electron–nucleus cusps for exact molecular wavefunctions. We report such an analysis elsewhere.[42] Our conclusion is that, although $\tau^{WF}(\mathbf{r})$, $\tau^{KS}(\mathbf{r})$, and $\tau_W(\mathbf{r})$ are indeed distinct and discontinuous in the basis-set limit, their directional dependence in the vicinity of a nucleus is nevertheless identical. This means that the discontinuities of the kinetic energy densities would cancel out exactly in a complete basis set to produce a continuous XC potential.

Discontinuities of XC potentials computed using finite STO basis sets may have practical implications. For instance, satisfying the electron–nucleus cusp condition is considered important in certain applications of electronic structure methods.[28,43–48] Although the true electron–nucleus cusps of molecular wavefunctions are not spherically symmetric, the electron–nucleus cusp conditions within STO basis sets are typically imposed on the spherically averaged values. The findings of Ref. 21 and this work suggest that this should be done carefully within STO basis sets, where quantities such as $\tau(\mathbf{r})$ do not have a single value at atomic nuclei.

V. CONCLUSION

We have shown that molecular XC potentials derived from electronic wavefunctions via Eqs. (1) and (3) using finite STO basis sets are discontinuous at the positions of the atomic nuclei. Equation (1) involves a difference in two different "positive-definite" kinetic energy densities, each of which is sharply discontinuous at atomic nuclei (Fig. 1). The discontinuities of $\tau^{WF}(\mathbf{r})$ and $\tau^{KS}(\mathbf{r})$ do not cancel out exactly, and the residual jump discontinuity shows up in the XC potential. Equation (3) involves a difference in Pauli kinetic energy densities whose discontinuities within STO basis sets are weaker but still do not cancel out completely. Thus, Eq. (3) also gives discontinuous XC potentials within finite STO basis sets, although to a lesser extent than Eq. (1).

If one accepts that the true (basis-set-limit) XC potentials are continuous at atomic nuclei, then Eqs. (1) and (3) imply that the jump discontinuities of $\tau^{WF}(\mathbf{r})$, $\tau^{KS}(\mathbf{r})$, and $\tau_W(\mathbf{r})$ must be identical to one another at each nucleus in a molecule. This conclusion is startling because these three quantities are quite different in general. Nevertheless, it can be proven rigorously.[42]

Within finite basis sets of cuspless GTOs, neither $\tau(\mathbf{r})$ nor $\tau_P(\mathbf{r})$ is discontinuous. That is why the formulas for $v_{XC}^{I}(\mathbf{r})$ and $v_{XC}^{II}(\mathbf{r})$ implemented using GTOs give continuous XC potentials

30 September 2024 16:01:33

Published under an exclusive license by AIP Publishing

automatically.[15,35] By contrast, finite STO basis sets produce XC potentials with spurious discontinuities. We arrive at a somewhat amusing conclusion: Although STOs work better than GTOs for describing wavefunctions near atomic nuclei, GTOs may be more suitable in situations where the subtle effects of electron–nucleus cusps must cancel out exactly.

ACKNOWLEDGMENTS

The work was supported by the Natural Sciences and Engineering Research Council of Canada (NSERC) through the Discovery Grants Program (Application No. RGPIN-2020-06420) and the Canada Graduate Scholarships Program (C.C.M.).

AUTHOR DECLARATIONS

Conflict of Interest

The authors have no conflicts to disclose.

Author Contributions

Conrad C. Moore: Conceptualization (equal); Funding acquisition (equal); Methodology (lead); Software (lead); Writing – original draft (lead). **Viktor N. Staroverov**: Conceptualization (equal); Funding acquisition (equal); Methodology (supporting); Writing – review & editing (lead).

DATA AVAILABILITY

The data that support the findings of this study are available within the article.

REFERENCES

[1]W. Kohn and L. J. Sham, "Self-consistent equations including exchange and correlation effects," Phys. Rev. **140**, A1133–A1138 (1965).
[2]G. E. Scuseria and V. N. Staroverov, "Progress in the development of exchange-correlation functionals," in *Theory and Applications of Computational Chemistry. The First Forty Years*, edited by C. E. Dykstra, G. Frenking, K. S. Kim, and G. E. Scuseria (Elsevier, Amsterdam, 2005), pp. 669–724.
[3]A. D. Kaplan, M. Levy, and J. P. Perdew, "The predictive power of exact constraints and appropriate norms in density functional theory," Annu. Rev. Phys. Chem. **74**, 193–218 (2023).
[4]R. G. Parr and W. Yang, *Density-Functional Theory of Atoms and Molecules* (Oxford University Press, New York, 1989).
[5]Q. Zhao, R. C. Morrison, and R. G. Parr, "From electron densities to Kohn–Sham kinetic energies, orbital energies, exchange-correlation potentials, and exchange-correlation energies," Phys. Rev. A **50**, 2138–2142 (1994).
[6]O. V. Gritsenko and E. J. Baerends, "Effect of molecular dissociation on the exchange-correlation Kohn–Sham potential," Phys. Rev. A **54**, 1957–1972 (1996).
[7]P. R. T. Schipper, O. V. Gritsenko, and E. J. Baerends, "Kohn–Sham potentials corresponding to Slater and Gaussian basis set densities," Theor. Chem. Acc **98**, 16–24 (1997).
[8]I. G. Ryabinkin and V. N. Staroverov, "Determination of Kohn–Sham effective potentials from electron densities using the differential virial theorem," J. Chem. Phys. **137**, 164113 (2012).
[9]A. A. Kananenka, S. V. Kohut, A. P. Gaiduk, I. G. Ryabinkin, and V. N. Staroverov, "Efficient construction of exchange and correlation potentials by inverting the Kohn–Sham equations," J. Chem. Phys. **139**, 074112 (2013).
[10]Y. Shi and A. Wasserman, "Inverse Kohn–Sham density functional theory: Progress and challenges," J. Phys. Chem. Lett. **12**, 5308–5318 (2021).
[11]M. A. Buijse, E. J. Baerends, and J. G. Snijders, "Analysis of correlation in terms of exact local potentials: Applications to two-electron systems," Phys. Rev. A **40**, 4190–4202 (1989).
[12]I. G. Ryabinkin, S. V. Kohut, and V. N. Staroverov, "Reduction of electronic wave functions to Kohn-Sham effective potentials," Phys. Rev. Lett. **115**, 083001 (2015).
[13]R. Cuevas-Saavedra, P. W. Ayers, and V. N. Staroverov, "Kohn–Sham exchange-correlation potentials from second-order reduced density matrices," J. Chem. Phys. **143**, 244116 (2015).
[14]R. Cuevas-Saavedra and V. N. Staroverov, "Exact expressions for the Kohn–Sham exchange-correlation potential in terms of wave-function-based quantities," Mol. Phys. **114**, 1050–1058 (2016).
[15]E. Ospadov, I. G. Ryabinkin, and V. N. Staroverov, "Improved method for generating exchange-correlation potentials from electronic wave functions," J. Chem. Phys. **146**, 084103 (2017).
[16]J. B. Stückrath and F. A. Bischoff, "Reduction of Hartree–Fock wavefunctions to Kohn–Sham effective potentials using multiresolution analysis," J. Chem. Theory Comput. **17**, 1408–1420 (2021).
[17]S. V. Kohut, A. M. Polgar, and V. N. Staroverov, "Origin of the step structure of molecular exchange-correlation potentials," Phys. Chem. Chem. Phys. **18**, 20938–20944 (2016).
[18]R. F. W. Bader and H. J. T. Preston, "The kinetic energy of molecular charge distributions and molecular stability," Int. J. Quantum Chem. **3**, 327–347 (1969).
[19]R. F. W. Bader and P. M. Beddall, "Virial field relationship for molecular charge distributions and the spatial partitioning of molecular properties," J. Chem. Phys. **56**, 3320–3329 (1972).
[20]Y. Tal and R. F. W. Bader, "Studies of the energy density functional approach. I. Kinetic energy," Int. Quantum. Chem. Symp. **14**(S12), 153–168 (1978).
[21]C. C. Moore and V. N. Staroverov, "Discontinuities of kinetic energy densities within finite and complete basis sets," J. Phys. Chem. A **128**, 6019–6025 (2024).
[22]T. Kato, "On the eigenfunctions of many-particle systems in quantum mechanics," Commun. Pure Appl. Math. **10**, 151–177 (1957).
[23]W. A. Bingel, "The behaviour of the first-order density matrix at the Coulomb singularities of the Schrödinger equation," Z. Naturforsch. A **18**, 1249–1253 (1963).
[24]R. T. Pack and W. Byers Brown, "Cusp conditions for molecular wavefunctions," J. Chem. Phys. **45**, 556–559 (1966).
[25]W. A. Bingel, "A physical interpretation of the cusp conditions for molecular wave functions," Theor. Chim. Acta **8**, 54–61 (1967).
[26]V. Sahni, *Quantal Density Functional Theory II: Approximation Methods and Applications* (Springer, Berlin, 2010), pp. 29–33.
[27]S. Liu, R. G. Parr, and A. Nagy, "Cusp relations for local strongly decaying properties in electronic systems," Phys. Rev. A **52**, 2645–2651 (1995).
[28]S. Tribedi, D.-K. Dang, B. Kanungo, V. Gavini, and P. M. Zimmerman, "Exchange correlation potentials from full configuration interaction in a Slater orbital basis," J. Chem. Phys. **159**, 054106 (2023).
[29]V. N. Staroverov and E. Ospadov, "Unified construction of Fermi, Pauli, and exchange-correlation potentials," Adv. Quantum Chem. **79**, 201–219 (2019).
[30]I. G. Ryabinkin, S. V. Kohut, R. Cuevas-Saavedra, P. W. Ayers, and V. N. Staroverov, "Response to "Comment on 'Kohn–Sham exchange-correlation potentials from second-order reduced density matrices' [J. Chem. Phys. **145**, 037101 (2016)]," J. Chem. Phys. **145**, 037102 (2016).
[31]Mathematica, Version 13.0, Wolfram Research, Inc., Champaign, IL, 2021.
[32]F. E. Harris, "Analytic evaluation of two-center STO electron repulsion integrals via ellipsoidal expansion," Int. J. Quantum Chem. **88**, 701–734 (2002).
[33]P. Pulay, "Improved SCF convergence acceleration," J. Comput. Chem. **3**, 556–560 (1982).
[34]I. Ema, J. M. García de la Vega, G. Ramírez, R. López, J. Fernández Rico, H. Meissner, and J. Paldus, "Polarized basis sets of Slater-type orbitals: H to Ne atoms," J. Comput. Chem. **24**, 859–868 (2003).
[35]I. G. Ryabinkin, E. Ospadov, and V. N. Staroverov, "Exact exchange-correlation potentials of singlet two-electron systems," J. Chem. Phys. **147**, 164117 (2017).

30 September 2024 16:01:33

Published under an exclusive license by AIP Publishing

[36]R. M. Dreizler and E. K. U. Gross, *Density Functional Theory* (Springer, Berlin, 1990), p. 110.
[37]G. Das and A. C. Wahl, "Extended Hartree–Fock wavefunctions: Optimized valence configurations for H_2 and Li_2, optimized double configurations for F_2," J. Chem. Phys. **44**, 87–96 (1966).
[38]F. Della Sala, E. Fabiano, and L. A. Constantin, "Kohn–Sham kinetic energy density in the nuclear and asymptotic regions: Deviations from the von Weizsäcker behavior and applications to density functionals," Phys. Rev. B **91**, 035126 (2015).
[39]A. Savin, F. Colonna, and R. Pollet, "Adiabatic connection approach to density functional theory of electronic systems," Int. J. Quantum Chem. **93**, 166–190 (2003).
[40]V. N. Staroverov, G. E. Scuseria, and E. R. Davidson, "Optimized effective potentials yielding Hartree–Fock energies and densities," J. Chem. Phys. **124**, 141103 (2006).
[41]Z. Qian, "Exchange and correlation near the nucleus in density functional theory," Phys. Rev. B **75**, 193104 (2007).
[42]C. C. Moore and V. N. Staroverov, "Are exact exchange-correlation potentials continuous at atomic nuclei in molecules?," J. Chem. Theory Comput. (in press).
[43]P. T. A. Galek, N. C. Handy, A. J. Cohen, and G. K.-L. Chan, "Hartree–Fock orbitals which obey the nuclear cusp condition," Chem. Phys. Lett. **404**, 156–163 (2005).
[44]A. Ma, M. D. Towler, N. D. Drummond, and R. J. Needs, "Scheme for adding electron-nucleus cusps to Gaussian orbitals," J. Chem. Phys. **122**, 224322 (2005).
[45]J. M. Garcia Lastra, J. W. Kaminski, and T. A. Wesolowski, "Orbital-free effective embedding potential at nuclear cusps," J. Chem. Phys. **129**, 074107 (2008).
[46]P. Reinhardt and P. E. Hoggan, "Cusps and derivatives for wave-functions expanded in Slater orbitals: A density study," Int. J. Quantum Chem. **109**, 3191–3198 (2009).
[47]J. Fernández Rico, R. López, I. Ema, and G. Ramírez, "Nuclear cusp conditions and their fulfillment in molecular calculations with SLATER basis sets," Int. J. Quantum Chem. **114**, 1393–1400 (2014).
[48]P.-F. Loos, A. Scemama, and M. Caffarel, "Self-consistent electron–nucleus cusp correction for molecular orbitals," Adv. Quantum Chem. **79**, 113–132 (2019).

30 September 2024 16:01:33

Published under an exclusive license by AIP Publishing